β-Ga_2O_3 MOSFETs for Radio Frequency Operation

Andrew Joseph Green, Kelson D. Chabak, Michele Baldini, Neil Moser, *Student Member, IEEE*, Ryan Gilbert, Robert C. Fitch, Jr., *Member, IEEE*, Günter Wagner, Zbigniew Galazka, Jonathan McCandless, *Member, IEEE*, Antonio Crespo, Kevin Leedy, and Gregg H. Jessen, Sr., *Member, IEEE*

***Abstract*— We demonstrate a β-Ga_2O_3 MOSFET with record-high transconductance (g_m) of 21 mS/mm and extrinsic cutoff frequency (f_T) and maximum oscillating frequency (f_{max}) of 3.3 and 12.9 GHz, respectively, enabled by implementing a new highly doped ohmic cap layer with a sub-micron gate recess process. RF performance was further verified by CW Class-A power measurements with passive source and load tuning at 800 MHz, resulting in P_{OUT}, power gain, and power-added efficiency of 0.23 W/mm, 5.1 dB, and 6.3%, respectively. These preliminary results indicate potential for monolithic or heterogeneous integration of power switch and RF devices using β-Ga_2O_3.**

***Index Terms*— β-Ga_2O_3, radio frequency, small-signal, large-signal, gate recess.**

I. Introduction

β-GA_2O_3 has recently seen significant attention as the next high performance power electronics material. The material's ultra-wide band gap of nearly 5 eV projects an electrical breakdown strength (E_C) of 8 MV/cm [1], [2]. While the breakdown strength is commonly applied to Baliga's figure of merit for unipolar power electronics [3], it also is a factor in Johnson's figure of merit (saturation velocity-critical electric field product, $v_{sat} \cdot E_c$), which is used to describe the power-frequency product for RF operation [4]. High voltage β-Ga_2O_3 MOSFET operation has already made large strides including E_C measurements greater than GaN or SiC's theoretical limit [5] and blocking voltages >600V for both enhancement [6] and depletion-mode [7] devices. With a measured mobility as high as 100 $cm^2/V{\cdot}s$ [8]–[11], an opportunity exists for β-Ga_2O_3 transistors to operate as an amplifier. This could have circuit level implications such as monolithic or heterogeneous device integration of high-efficiency RF amplifiers, RF switches, and power switches capable of GHz switching speeds. Here, we demonstrate the first RF operation of a β-Ga_2O_3 MOSFET.

It has recently been shown that β-Ga_2O_3 can be doped to degenerate levels with donor concentrations greater than 1×10^{19} cm^{-3} [8], [12]–[15]. In light of this, a highly doped capping layer was grown on a lower doped β-Ga_2O_3 MOSFET transistor channel permitting the combination of low ohmic contact resistance and adequate channel control with a shorter gate length through a gate recess process. These design improvements combined with improved crystalline perfection of the β-Ga_2O_3 layer enabled power gain measurements in both small and large signal RF operation. We highlight a cutoff frequency (f_T) and maximum oscillating frequency (f_{MAX}) of 3.3 GHz and 12.9 GHz, respectively, and output power (P_{OUT}) of 0.23 W/mm with a power added efficiency (PAE) of 6.3% at 800 MHz using passive source and load tuning. Specifics of the transistor design and additional RF results are presented below.

II. Device Fabrication

A Si-doped β-Ga2O3 layer was homoepitaxially grown by metalorganic vapor phase epitaxy (MOVPE) on a semi-insulating (100) substrate, as described in prior work [15]. The substrate was cut from a two-inch boule grown via the Czochralski method [16] with a misorientation of 6° towards the [001] direction that promotes step-flow growth and dramatically decrease the density of planar defects in the layer [17]. The channel and ohmic cap layers were grown with target thickness and donor concentrations of 180 nm/$1 \times 10^{18} cm^{-3}$ and 25 nm/$1 \times 10^{19} cm^{-3}$, respectively. Device isolation was performed with an inductively coupled plasma/reactive ion etch (ICP/RIE) using BCl_3 chemistry. Source and drain ohmic contacts were formed using an evaporated Ti/Al/Ni/Au metal stack and observed to be ohmic after annealing for 60 s in a nitrogen ambient at 470 °C. The highly doped β-Ga_2O_3 capping layer was removed in the channel by a second ICP/RIE etch in BCl_3. A 200 nm SiO_2 layer was then deposited by plasma enhanced chemical vapor deposition to act as both a passivation and field plate separation layer. A 0.7 μm gate recess was patterned and etched into the SiO_2 by RIE to form the gate foot geometry. Immediately following the SiO_2 etch, a third BCl_3 etch was used to create the gate recess. Nearly

Manuscript received March 27, 2017; revised April 10, 2017; accepted April 10, 2017. Date of publication April 19, 2017; date of current version May 22, 2017. This work was supported by the Air Force Research Laboratory. The review of this letter was arranged by Editor M. Tabib-Azar. *(Corresponding author: Andrew Joseph Green.)*

A. J. Green, R. Gilbert, and J. McCandless are with Wright-Patterson Air Force Base, AFRL, Dayton, OH 45433 USA, and also with KBRwyle, Dayton, OH 45433 USA (e-mail: andrew.green.16.ctr@us.af.mil).

K. D. Chabak, R. C. Fitch, Jr., A. Crespo, K. Leedy, and G. H. Jessen, Sr., are with Wright-Patterson Air Force Base, AFRL, Dayton, OH 45433 USA.

M. Baldini, G. Wagner, and Z. Galazka are with the Leibniz Institute for Crystal Growth, IKZ, 12489 Berlin, Germany.

N. Moser is with the Department of Electrical and Computer Engineering, George Mason University, Fairfax, VA 22030 USA.

Digital Object Identifier 10.1109/LED.2017.2694805

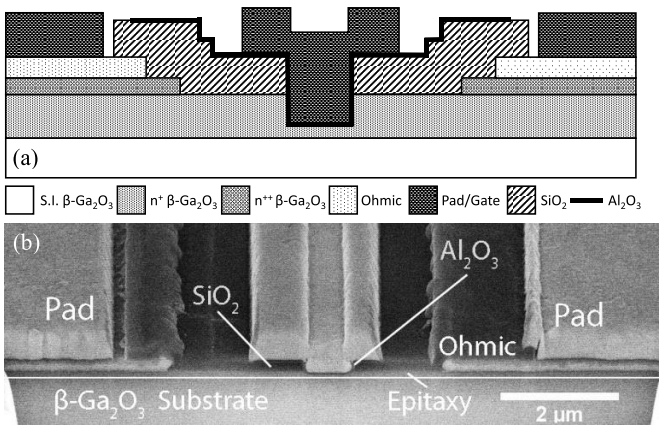

Fig. 1. (a) A device cross section schematic is shown for the β-Ga_2O_3 MOSFET under test. (b) A focused ion beam (FIB) cross sectional image of the device. This is the bottom finger of the 2 × 50 μm split finger device.

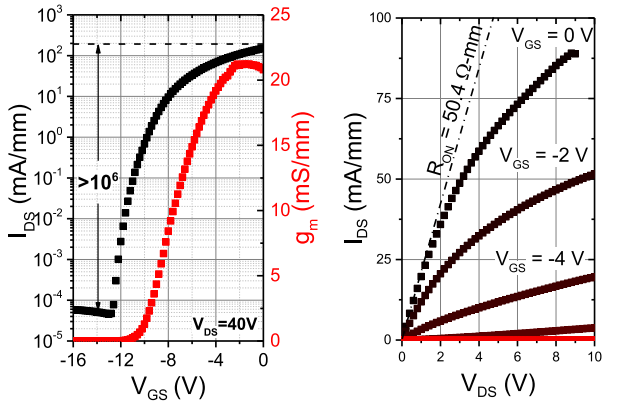

Fig. 2. (a) DC transfer characteristics for a 2 × 50 μm β-Ga_2O_3 gate recessed MOSFET. I_{ON}/I_{OFF} and I_{DMAX} at V_{GS} = 0V were measured to be $>10^6$ and 150 mA/mm, respectively. (b) Family of output curves for the same device in (a). The gate bias step is −2 V starting at 0V. A normalized R_{ON} of 50.4 Ω · mm was measured.

half of the original channel layer was etched leaving ∼90 nm of epitaxy as measured by surface profilometry. A 20 nm thick Al_2O_3 layer was then deposited via thermal atomic layer deposition (ALD) for the gate dielectric. Both SiO_2 and Al_2O_3 were then etched with CF_4 based RIE in pad regions over the ohmic contacts. Afterwards, interconnect and gate metal stacks consisting of Ni/Au were simultaneously evaporated. Finally, 2 μm of thick interconnect metal (Ti/Au) was evaporated facilitating extra current handling capability.

Test structures with the thin ohmic cap layer etched away were available for process control monitoring. The post-processed carrier concentration and mobility were measured via the Hall Effect on van der Pauw (VDP) structures to be 1.3 × 10^{18} cm^{-3} and 96 cm^2/V·s, respectively. A nearby transfer length measurement (TLM) structure was used to determine the contact and sheet resistance, they were measured to be 3.3 Ω·mm and 4850 Ω/sq, respectively. A focused-ion beam (FIB) cross section of the measured 2 × 50 μm device can be seen in Fig. 1b. The transistor channel is defined by the ohmic cap etch boundary resulting in a source-drain spacing (L_{SD}), gate-drain spacing (L_{GD}), and gate length (L_G) of 3.8 μm, 1.6 μm, and 0.7 μm, respectively.

III. DC and RF Performance

Standard DC transfer characteristics were measured as shown in Fig 2. The maximum current density was 150 mA/mm at $V_{GS} = 0$ and $V_{DS} = 40$V. The I_{ON}/I_{OFF} ratio was greater than 10^6. The threshold voltage was extrapolated to be -10.1 V from a linear fit to the transconductance curve. The maximum transconductance is 21.2 mS/mm, approximately 7 times greater than the best previously reported depletion mode MOSFET [5] and higher than any other published result for β-Ga_2O_3 [7], [18]. A family of output curves was collected starting at $V_G = 0$ with a gate bias step of −2V. The drain contact was limited to 10 V to protect the device while observing device linearity. The normalized on-resistance (R_{ON}) was measured to be 50.4 Ω·mm from a linear fit to the $V_{GS} = 0$V curve.

Extrinsic small signal RF gain performance was recorded at a drain voltage of $V_{DS} = 40$V and the gate electrode

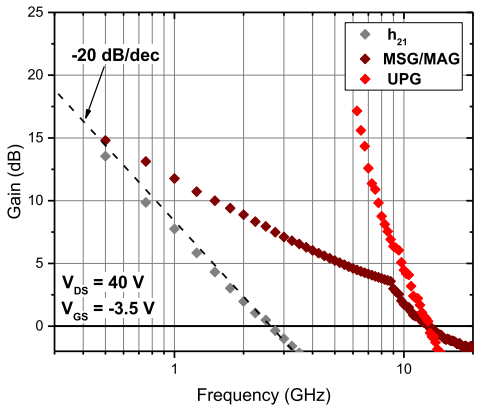

Fig. 3. Extrinsic small signal RF gain performance recorded at $V_{GS} = -3.5$ V (peak g_m) and $V_{DS} = 40$V. A gain decay of −20 dB/dec is plotted with the dashed line.

biased at the peak transconductance voltage ($V_{GS} = -3.5$ V). Fig. 3 shows forward current gain (h_{21}), maximum stable gain/maximum available gain (*MSG/MAG*), and unilateral power gain (*UPG*) calculated from the scattering parameters (S-parameters) and plotted as a function of frequency. A cutoff frequency (f_T) and maximum oscillating frequency (f_{MAX}) were measured to be 2.7 GHz and 12.9 GHz, respectively ($V_{DS} = 40$V).

Figure 4 shows f_T and f_{MAX} as a function of drain voltage from 10V to 40V with a 5V step. The gate voltage was set to the peak transconductance value for each small signal measurement. The f_T changed slightly across the drain voltage sweep and peaked at 3.3 GHz. The f_{MAX} increased significantly as a function of drain voltage and began to saturate around 35V. The maximum f_{MAX} value measured was 12.9 GHz at a drain bias of 40V.

Large signal CW RF operation was also measured on the same device. An input power sweep was performed at 800 MHz with V_{DS} and V_{GS} set to 25 V and −4V, respectively (approximating Class A operation), following passive source and load tuning for maximum output power. The P_{OUT} was measured to be 13.7 dBm, or 0.23 W/mm. Both

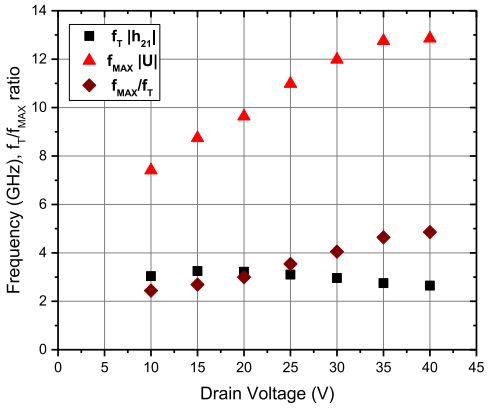

Fig. 4. Cutoff frequency (f_T) and maximum oscillating frequency (f_{MAX}) as a function of drain bias. Each measurement was taken with the gate contact biased with the gate voltage corresponding to peak transconductance.

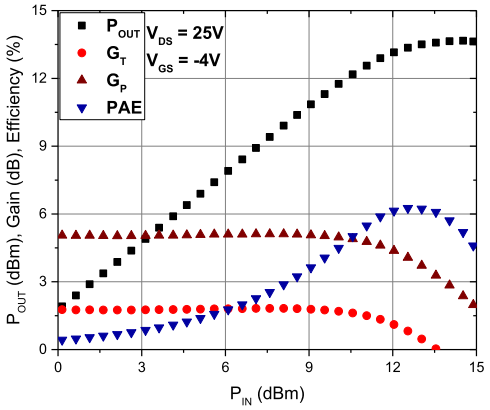

Fig. 5. 800 MHz Class-A power sweep of a 2 × 50 μm β-Ga_2O_3 gate recessed MOSFET.

small and large signal measurements had significant reflected power due to a large high input impedance (small device periphery of 100 μm coupled with a large sheet resistance of 4850 Ω/□) of the device which could not be properly matched at the source side. To quantify this effect, a power sensor was attached to a source side directional coupler to measure the reflected power from port 1. This was subtracted from P_{IN} to calculate the device power gain (G_P). Transducer gain (G_T), by definition was not adjusted for the reflected power. P_{OUT}, PAE, G_T and G_P are plotted as a function of input power (P_{IN}) in Fig 5. We measured a maximum G_T and G_P of 1.8 dB and 5.1 dB, respectively. Additional power sweeps were conducted with increasing drain bias as high as 50 V to achieve 0.25 W/mm with only 1.4% PAE. However, this eventually lead to catastrophic failure of the device from thermal effects where the operating temperature is expected to exceed 300 °C under these test conditions. It is suspected that the significant device heating has adverse effects on large signal performance. Degradation of the device characteristics was observed prior to the catastrophic failure. These early results indicate promising RF potential for β-Ga_2O_3 MOSFETs as crystallinity improves and device scaling techniques are implemented. Additionally, dramatic improvements are expected with heterostructure development [19], [20].

IV. Conclusions

Reported here is a first look into the RF performance of a β-Ga_2O_3 MOSFET. The RF result is achieved through the reduction of contact resistance, due to a highly doped cap layer, and through the use of a gate recess, allowing for gate length scaling. DC transfer measurements showed a high current density and transconductance of 150 mA/mm and 21.2 mS/mm, respectively. Extrinsic small signal RF operation was verified with f_T and f_{MAX} measured to be 3.3 GHz and 12.9 GHz, respectively. Large signal operation was also measured on the same device at 800 MHz corresponding to G_T and G_P gains of 1.8 dB and 5.1 dB, respectively. A maximum value of P_{OUT} was measured to be 13.7 dBm which translates to 0.23 W/mm. Finally, the maximum PAE was measured to be 6.3%. RF performance is expected to substantially improve with device optimization and materials development.

References

[1] M. Higashiwaki, K. Sasaki, T. Kamimura, M. H. Wong, D. Krishnamurthy, A. Kuramata, T. Masui, and S. Yamakoshi, "Depletion-mode Ga_2O_3 metal-oxide-semiconductor field-effect transistors on β-Ga_2O_3 (010) substrates and temperature dependence of their device characteristics," *Appl. Phys. Lett.*, vol. 103, pp. 1–4, Sep. 2013, doi: 10.1063/1.4821858.

[2] M. Higashiwaki, K. Sasaki, A. Kuramata, T. Masui, and S. Yamakoshi, "Gallium oxide (Ga_2O_3) metal-semiconductor field-effect transistors on single-crystal β-Ga_2O_3 (010) substrates," *Appl. Phys. Lett.*, vol. 100, pp. 1–2, Jan 2 2012, doi: 10.1063/1.3674287.

[3] B. J. Baliga, "Semiconductors for high-voltage, vertical channel field-effect transistors," *J. Appl. Phys.*, vol. 53, pp. 1759–1764, Sep. 1982, doi: 10.1063/1.331646.

[4] E. O. Johnson, "Physical limitations on frequency and power parameters of transistors," *RCA Rev.*, vol. 26, p. 163, Oct. 1965, doi: 10.1109/IRECON.1965.1147520.

[5] A. Green, K. Chabak, E. Heller, R. Fitch, M. Baldini, A. Fiedler, K. Irmscher, G. Wagner, Z. Galazka, S. Tetlak, A. Crespo, K. Leedy, and G. Jessen, "3.8 MV/cm breakdown strength of MOVPE-grown Sn-doped β-Ga_2O_3 MOSFETs," *IEEE Electron Device Lett.*, vol. 37, no. 7, pp. 902–905, Jul. 2016, doi: 10.1109/LED.2016.2568139.

[6] K. Chabak, N. Moser, A. Green, D. Walker, S. Tetlak, E. Heller, A. Crespo, R. Fitch, J. McCandless, K. Leedy, X. Li, and G. Jessen, "Enhancement-mode Ga_2O_3 wrap-gate fin field-effect-transistors on native (100) β-Ga_2O_3 substrate with high breakdown voltage," *Appl. Phys. Lett.*, vol. 109, p. 213501, Nov. 2016, doi: 10.1063/1.4967931.

[7] M. H. Wong, K. Sasaki, A. Kuramata, S. Tamakoshi, and M. Higashiwaki, "Field-plated Ga_2O_3 MOSFETs with a breakdown voltage of over 750 V," *IEEE Electron Device Lett.*, vol. 37, no. 2, pp. 212–215, Feb. 2016, doi: 10.1109/LED.2015.2512279.

[8] K. Sasaki, A. Kuramata, T. Masui, E. G. Villora, K. Shimamura, and S. Yamakoshi, "Device-quality β-Ga_2O_3 epitaxial films fabricated by ozone molecular beam epitaxy," *Appl. Phys. Exp.*, vol. 5, pp. 1–3, Mar. 2012, doi: 10.1143/apex.5.035502.

[9] N. Ma, N. Tanen, A. Verma, Z. Guo, T. Luo, H. G. Xing, and D. Jena, "Intrinsic electron mobility limits in β-Ga_2O_3," *Appl. Phys. Lett.*, vol. 109, p. 212101, Nov. 2016, doi: 10.1063/1.4968550.

[10] K. Irmscher, Z. Galazka, M. Pietsch, R. Uecker, and R. Fornari, "Electrical properties of β-Ga_2O_3 single crystals grown by the Czochralski method," *J. Appl. Phys.*, vol. 110, pp. 1–7, Sep. 2011, doi: 10.1063/1.3642962.

[11] T. Oishi, Y. Koga, K. Harada, and M. Kasu, "High-mobility β-Ga_2O_3(201) single crystals grown by edge-defined film-fed growth method and their Schottky barrier diodes with Ni contact," *Appl. Phys. Exp.*, vol. 8, pp. 1–3, Mar. 2015, doi: 10.7567/apex.8.031101.

[12] K. Sasaki, M. Higashiwaki, A. Kuramata, T. Masui, and S. Yamakoshi, "Si-Ion implantation doping in β-Ga_2O_3 and its application to fabrication of low-resistance ohmic contacts," *Appl. Phys. Exp.*, vol. 6, p. 086502, Aug. 2013, doi: 10.7567/apex.6.086502.

[13] F. B. Zhang, K. Saito, T. Tanaka, M. Nishio, and Q. X. Guo, "Electrical properties of Si doped Ga_2O_3 films grown by pulsed laser deposition," *J. Mater. Sci.-Mater. Electron.*, vol. 26, pp. 9624–9629, Dec. 2015, doi: 10.1007/s10854-015-3627-6.

[14] K. Zeng, J. Wallace, C. Heimburger, K. Sasaki, A. Kuramata, T. Masui, J. Gardella, and U. Singisetti, "Ga_2O_3 MOSFETs using spin-on-glass source/drain doping technology," *IEEE Electron Device Lett.*, vol. 38, no. 4, pp. 513–516, Apr. 2017, doi: 10.1109/LED.2017.2675544.

[15] M. Baldini, M. Albrecht, A. Fiedler, K. Irmscher, R. Schewski, and G. Wagner, "Si- and Sn-doped homoepitaxial β-Ga_2O_3 layers grown by MOVPE on (010)-oriented substrates," *Ecs J. Solid State Sci. Technol.*, vol. 6, no. 2, pp. Q3040–Q3044, 2017, doi: 10.1149/2.0081702jss.

[16] Z. Galazka, K. Irmscher, R. Uecker, R. Bertram, M. Pietsch, A. Kwasniewski, M. Naumann, T. Schulz, R. Schewski, D. Klimm, and M. Bickermann, "On the bulk β-Ga_2O_3 single crystals grown by the Czochralski method," *J. Cryst. Growth*, vol. 404, pp. 184–191, Oct. 2014, doi: 10.1016/j.jcrysgro.2014.07.021.

[17] R. Schewski, M. Baldini, K. Irmscher, A. Fiedler, T. Markurt, B. Neuschulz, T. Remmele, T. Schulz, G. Wagner, Z. Galazka, and M. Albrecht, "Evolution of planar defects during homoepitaxial growth of β-Ga_2O_3 layers on (100) substrates-A quantitative model," *J. Appl. Phys.*, vol. 120, no. 22, p. 225308, Dec. 2016, doi: 10.1063/1.4971957.

[18] H. Zhou, M. W. Si, S. Alghamdi, G. Qiu, L. M. Yang, and P. D. Ye, "High-performance depletion/enhancement-mode β-Ga_2O_3 on insulator (GOOI) field-effect transistors with record drain currents of 600/450 mA/mm," *IEEE Electron Device Lett.*, vol. 38, no. 1, pp. 103–106, Jan. 2017, doi: 10.1109/led.2016.2635579.

[19] Y. Oshima, E. Ahmadi, S. C. Badescu, F. Wu, and J. S. Speck, "Composition determination of β-$(Al_xGa_{1-x})_2O_3$ layers coherently grown on (010) β-Ga_2O_3 substrates by high-resolution X-ray diffraction," *Appl. Phys. Exp.*, vol. 9, no. 6, p. 061102, Jun. 2016, doi: 10.7567/apex.9.061102.

[20] O. Takayoshi, K. Yuji, K. Naoto, K. Akito, Y. Shigenobu, F. Shizuo, O. Toshiyuki, and K. Makoto, "Carrier confinement observed at modulation-doped β-$(Al_xGa_{1-x})_2O_3$/Ga_2O_3 heterojunction interface," *Appl. Phys. Exp.*, vol. 10, no. 3, p. 035701, 2017, doi: 10.7567/APEX.10.035701.